https://doi.org/10.5194/egusphere-2023-1483
Preprint. Discussion started: 25 July 2023

Formation of particulate organic carbon from dissolved substrate input enhances soil carbon sequestration

Qintana Si[1], Kangli Chen[1], Bin Wei[1], Yaowen Zhang[1], Xun Sun[1], Junyi Liang[1]

[1]Department of Grassland Resource and Ecology, College of Grassland Science and Technology, China Agricultural University, Beijing 100193, China

Correspondence to: Junyi Liang (+86 10 62733381; liangjunyi@cau.edu.cn)

Abstract. Particulate organic carbon (POC) and mineral-associated organic carbon (MAOC), which are two primary components of the soil carbon (C) reservoir, have different physical and chemical properties and biochemical turnover rates. Microbial necromass entombment is a primary mechanism for MAOC formation from fast-decaying plant substrates, whereas POC is typically considered as the product of structural litter via physical fragmentation. However, emerging evidence shows that microbial by-products derived from labile C substrates can enter the POC pool. To date, it is still unclear to what extent labile substrates contribute to the POC formation and the subsequent long-term SOC stock. Our study here, through a ^{13}C-labeling experiment in 10 soils from 5 grassland sites as well as a modeling analysis, showed that up to 12.29% of isotope-labeled glucose-C (i.e., dissolved C) was detected in POC pool. In addition, the glucose-derived POC was dependent upon ^{13}C-MBC and the fraction of clay and silt, suggesting that the POC formation from newly added labile C is dependent on interactions between soil physical and microbial processes. The modeling analysis showed that ignoring the C flow from MBC to POC significantly underestimated soil C sequestration by 7.79% – 49.51% across the 10 soils. The results emphasize that the soil texture-regulated microbial process, besides the plant structural residues, is a significant contributor to POC, acting as a vital component in SOC dynamics.

Keywords: soil carbon sequestration, soil carbon modeling, particulate organic carbon, dissolved organic carbon, soil carbon input, glucose

https://doi.org/10.5194/egusphere-2023-1483
Preprint. Discussion started: 25 July 2023

1 Introduction

As the largest terrestrial carbon (C) pool, soil organic C (SOC) plays a vital role in regulating global climate change through C emissions and sequestration (White et al., 2000; Chapin et al., 2011; Wiesmeier et al., 2019; Basile-Doelsch et al., 2020; Bai and Cotrufo, 2022). Carbon from root exudates and plant residues can be stabilized in the form of mineral-associated organic C (MAOC) or particulate organic C (POC), which have different features (Cotrufo et al., 2019; Sokol et al., 2019b; Lavallee et al., 2020). MAOC is generally small molecular organo-mineral complexes with relatively low C/nitrogen (N) ratios (C/N ratios). Being associated with minerals and occluded in the silt- and clay-sized aggregates, MAOC has a longer mean residence time than POC and thus is considered the key to long-term soil sequestration (Baldock and Skjemstad, 2000). As opposed to this, POC is usually considered as the product of physically fragmented structural residues and is more susceptible to external environmental changes (Benbi et al., 2014; Lugato et al., 2021). Although roughly dividing SOC into POC and MAOC is relatively easy to operate, the microbe-mediated SOC dynamics is a continuous process, making it is difficult to completely separate its biochemical and physical processes (Lehmann et al., 2020). During the gradual decomposition of plant residues, POC encapsulated by microbial by-products can bind silt- and clay-sized soil minerals, forming heavy-POC (or course-MAOC, >53 μm and >1.6 – 1.85 g cm^{-3}) (Samson et al., 2020). Since heavy-POC is the hotspot of microbial activities and microaggregates formation, it could also be a precursor of MAOC (Prater et al., 2020; Witzgall et al., 2021; Robertson et al., 2019).

Dissolved C input from living root, which has dominant effect on net formation of SOC, is considered approximately 2 to 13 times more efficient than litter inputs in forming SOC (Sokol et al., 2019b; Cotrufo et al., 2013). It is commonly believed that small-molecular labile plant substrates – such as glucose and other dissolved C – are primary sources of MAOC through physical absorption and microbial *in vivo* turnover via cell uptake-biosynthesis-growth-death (Kleber et al., 2015; Bai and Cotrufo, 2022; Mikutta et al., 2019; Sokol et al., 2019a; Liang et al., 2017). However, it has been paid much less attention how much microbial products derived from labile C may stick to semi-decomposed plant residues and connect with soil minerals to become part of POC.

As an important component of SOC, POC is pivotal to predict SOC sequestration. Although a few mechanistic models propose the POC formation from microbial metabolism, understanding of factors that control the POC formation is limited (Li et al., 2014; Robertson et al., 2019; Cotrufo and Lavallee, 2022). Specifically, direct evidence is still lacking to what extent dissolved substrate (e.g., glucose) contributes to POC formation. Additionally, how the dissolved substrates-originated POC formation affects SOC sequestration is rarely studied. In this study, we first conducted an incubation experiment by adding ^{13}C-labeled glucose solution to 10 soils from 5 grassland sites. At the end of experiment, glucose-derived ^{13}C in dissolved organic C (DOC), microbial biomass C (MBC), POC and MAOC were assessed. Then, we conducted a modeling experiment to simulate SOC dynamics at different C addition scenarios with and without a C flow from MBC to POC. This study was to answer the following three questions: (i) to what extent the added glucose contributes to the formation of POC? (ii) what factors control the POC formation from glucose? (iii) how does dissolved substrates-originated POC formation affect SOC sequestration?

https://doi.org/10.5194/egusphere-2023-1483
Preprint. Discussion started: 25 July 2023

2 Materials and Methods

2.1 Soil sampling

In August 2021, 10 soils were sampled from 5 temperate grasslands of the Inner Mongolian Plateau, China (Table 1). At each site, soils of the top 20 cm layer were sampled from continuous grazing grassland and grazing excluded grassland, respectively. Before incubation, all soil samples were passed through a 2 mm sieve to remove visible stones, roots, and other plant debris. After homogenization, soil texture, pH, SOC, MBC and DOC content were measured (See methods below; Table 1). All soil samples were stored at -20 °C until the incubation experiment started.

2.2 Incubation experiment

For each soil, ^{13}C-labeled glucose addition treatments were performed and four replicates were conducted. Soil samples equivalent to 20 g air-dried soil were added to 250 ml mason jars. All soils were incubated in the dark at 25 °C and a relative humidity of 60% for 102 days. To maintain soil moisture at 60% water holding capacity (WHC), we added distilled water regularly by measuring the weight changes of the jars which were covered by a sealing film passable for gases but not water molecules. After a 7-day pre-incubation, ^{13}C-labeled glucose (99 atom% ^{13}C, Shanghai Engineering Research Center of Stable Isotope) at a dose of 0.4 mg C g^{-1} soil was added. On day 1, 3, 6, 12, 19, 34, 47, 78, and 102 of the incubation, each jar was flushed by CO_2-free air for 3 minutes. After that, CO_2 efflux was measured using an infrared gas analyzer (Li-8100A; Li-COR, USA) within 3 minutes from the headspace. After the last gas measurement, soils were destructively harvested and stored at -80°C for the subsequent measurements.

2.3 Measurements of DOC, MBC, POC and MAOC

The chloroform-fumigation-extraction method was used to determine DOC and MBC contents (Vance et al., 1987). One subsample of 5 g fresh soil was fumigated by chloroform in the dark for 24h and a second subsample (5g) was unfumigated as the control. Soil microbes died after 24 hours of chloroform fumigation, and their cells lysed and released microbial biomass C. The soil was extracted with 0.5M K_2SO_4 solution subsequently. The dissolved C in the extracting solution was determined by a rapid CS analyzer (Multi N/C 3100, Analytik jena, Germany). The DOC content was calculated according to the organic C content of unfumigated soil. The MBC content was the difference of DOC between fumigated and unfumigated soils multiplying by the proportionality coefficient of 0.45.

The POC and MAOC content were assessed through the particle size fractionation method, which separates SOC into these two pools. Soil samples (10g) were shaken with 30 mL of sodium hexametaphosphate solution (NaHMP, 50 g L^{-1}) at 200 rpm. After 18h, samples were washed with deionized water over a 53 μm sieve in a vibratory shaker (AS 200 control, Retch, Germany). Both fractions were dried at 65 °C, weighed, and fumigated with hydrochloric acid for 8h to remove inorganic C. Organic C content was determined by an elemental analyzer (rapid CS cube, elementar, Germany). The C from less than 53 μm fraction was considered MAOC, and the other was POC.

https://doi.org/10.5194/egusphere-2023-1483
Preprint. Discussion started: 25 July 2023

2.4 ^{13}C partitioning

To analyze the MBC-^{13}C concentration, an 8-ml extracting solution from each fumigated and unfumigated soil was freeze-dried, and approximately 8 mg of K_2SO_4-C was analyzed using an Isotope Ratio Mass Spectrometer (Delta V Advantage, ThermoFisher Scientific, America). The atom% of MBC in control and treated soils was determined using a two-pool mixing model:

$$at\%_{MBC} = \frac{at\%_{fumigated} \cdot C_{fumigated} - at\%_{unfumigated} \cdot C_{unfumigated}}{C_{fumigated} - C_{unfumigated}} , \quad (1)$$

where $C_{fumigated}$ and $C_{unfumigated}$ are the C mass in fumigated and unfumigated samples, and $at\%_{fumigated}$ and $at\%_{unfumigated}$ are the C isotope abundance (in atom% ^{13}C) of the fumigated and non-fumigated samples, respectively.

To analyze the content of POC-^{13}C and MAOC-^{13}C, approximately 2 mg of wet-sieved and oven-dried soil samples were determined by the Isotope Ratio Mass Spectrometer. Further, the contributions of glucose-derived C to DOC, MBC, POC, and MAOC pools were estimated following the isotopic mixing model:

$$C_{glucose-derived} = C_{total} \cdot \frac{at\%_{treatment} - at\%_{soil}}{at\%_{glucose} - at\%_{soil}} , \quad (2)$$

$$C_{soil} = C_{total} - C_{glucose-derived} , \quad (3)$$

Where $at\%_{treatment}$, $at\%_{soil}$, $at\%_{glucose}$ are the C isotope compositions (in atom% ^{13}C) of the glucose-treated soil, original soil, and added glucose, respectively; $C_{glucose-derived}$, C_{soil} and C_{total} are the glucose-derived, soil-derived C and total SOC content (mg C g^{-1} soil) in the glucose-treated soil, respectively.

2.5 Modeling analysis

The SOC dynamics was simulated using two mechanistic models. Most parts of the two models were identical except that Model I did not include the C flow from MBC to POC, but Model II did (Fig. 1). Model I assumed that plant structural residues were the only POC source, whereas Model II assumed that POC could be from both plant and microbial residues. Thus, dissolved C can be transformed to POC via microbial metabolism in Model II. The two models shared similar structure:

$$\frac{dX(t)}{dt} = AKX(t) , \quad (4)$$

where

$$X(t) = \begin{bmatrix} x_D \\ x_B \\ x_P \\ x_M \end{bmatrix} , \quad (5)$$

and

https://doi.org/10.5194/egusphere-2023-1483
Preprint. Discussion started: 25 July 2023

$$K = \begin{bmatrix} k_D & & & \\ & k_B & & \\ & & k_P & \\ & & & k_M \end{bmatrix}, \quad (6)$$

In Model I,

$$A = \begin{bmatrix} -1 & & f_{DP} & f_{DM} \\ f_{BD} & -1 & & \\ & & -1 & \\ & f_{MB} & f_{MP} & -1 \end{bmatrix}, \quad (7)$$

whereas in Model II

$$A = \begin{bmatrix} -1 & & f_{DP} & f_{DM} \\ f_{BD} & -1 & & \\ & f_{PB} & -1 & \\ & f_{MB} & f_{MP} & -1 \end{bmatrix}, \quad (8)$$

In matrix X, x_D, x_B, x_P, x_M are the pool sizes of DOC, MBC, POC and MAOC, and k_D, k_B, k_P, k_M in matrix K are their turnover rates, respectively. In matrix A, f_{BD} means the fraction transfer from the DOC pool to the MBC pool, other transfer coefficients f represent in the same way (See details in Table 2). The measured DOC and MBC before incubation were used as their respective initial pool sizes, whereas a to-be-determined parameter f_P was used to represent the initial fraction of POC – i.e., $initial\ POC = (SOC - DOC - MBC) \times f_p$. Correspondingly, the initial MAOC pool size was calculated as $(SOC - DOC - MBC) \times (1 - f_p)$. Overall, Model I had 10 and Model II had 11 to-be-determined parameters (Table 2). Because the glucose addition was ^{13}C-labelled, each C pool was further divided into soil-derived and glucose-derived pools. We considered all glucose addition entered the glucose-derived DOC pool in the beginning.

The models were calibrated using the incubation experiment through the adaptive Metropolis algorithm (Haario et al., 2001; Hararuk et al., 2014). The prior probability density functions (PDFs) were assumed as uniform distributions over parameter ranges based on previous studies (Li et al., 2014; Liang et al., 2015). The parameters' posterior PDFs were proportional to the prior PDFs and a cost function from data. The cost function was calculated as:

$$P(Z \mid \theta) \propto \exp\left\{-\sum_{t\in \mathrm{obs(Z)}} \frac{[\mathrm{O}_f(t)-\mathrm{M}_f(t)]^2}{2{\sigma_f}^2(t)} - \sum_{i\in \mathrm{obs(Z)}} \frac{[\mathrm{O}_p(i)-\mathrm{M}_p(i)]^2}{2{\sigma_p}^2(i)}\right\}, \quad (9)$$

where t denotes the measurement time of fluxes and i denotes C pools. σ^2 is the standard deviation of measurements. O_f and M_f are the observed and modelled respiration fluxes. O_p and M_p are the observed and modelled values of C pools. After the model calibration, we randomly select 100 sets of parameters for further modeling experiments. For each model, we set up two C input scenarios, DOC input only and DOC+POC input. The amount of C input was approximately equivalent to local annual C influxes (Table S1). The calibrated models were run to the steady states to compare the modelled SOC change

https://doi.org/10.5194/egusphere-2023-1483
Preprint. Discussion started: 25 July 2023

under different scenarios. After that, the models were run along a gradient of C input increase from 1% to 20% with a 1% interval to reach another steady state. Then the impact of C flow from MBC to POC (i.e., f_{PB}) on long-term SOC sequestration was assessed by comparing the behaviors of SOC dynamics between Model I and Model II.

2.6 Statistical analysis

The two-way analysis of variance (ANOVA) was used to reveal the effects of effects of sites, fencing, and their interaction on glucose-derived SOC, MAOC, POC, MBC, and DOC (Table S2). The differences caused by f_{PB} between Model I and Model II were tested using the one-way ANOVA. All data were separately tested for normality using the Shapiro–Wilk test and for homoscedasticity using the Bartlett's test in advance. In cases where the assumptions of normality or homoscedasticity were not met, a reciprocal transformation was applied to the original data, and analyses were carried out on the transformed data. In cases where the reciprocal transformed data did not meet the test requirements, the Kruskal-Wallis test was applied. The difference was considered statistically significant at the level of $P < 0.05$. The statistical was analyses were performed in R 4.1.2. The model was performed in Matlab 2021a.

3 Results

Across the 10 soils, 84.28 –175.80 mg kg^{-1} soil of the glucose C stayed in the soil after 102 days' incubation, with significant effects of site and fencing (Table S2, Fig. S1). Specifically, glucose-derived MBC, MAOC and POC were 18.68 – 51.44, 59.96 – 100.11 and 1.33 – 49.14 mg kg^{-1} soil, respectively (Fig. 2). Additionally, glucose-derived MAOC and POC were dependent upon glucose-derived MBC (Fig. 3a). Furthermore, glucose-derived MAOC and POC increased with the fraction of clay and silt (R^2 = 0.62 and 0.92, respectively, Fig. 3b).

The estimated C pool turnover rates were lower but the transfer coefficients among different C pools were greater in Model I than Model II (Table S3). On average, Model I underestimated k_D by 2.15%, k_B by 11.9%, k_P by 7.13%, k_M by 5.08%, whereas overestimated f_{MB} by 2.36%, f_{MP} by 4.47%, f_{DP} by 1.23%, f_{DM} by 2.77%, f_{BD} by 0.67%. Although both models fitted respiration flux data well (Fig. S2), Model I, without the C flow from MBC to POC, was not able to reproduce the observed glucose-derived POC (Fig. S3).

At the steady state, when C input only included DOC, SOC content in Model I was 19.54% – 49.51% less than that in Model II ($P < 0.05$; Fig. 4). When C input was from both DOC and POC, excluding the C flow from MBC to POC decreased SOC by 7.79% – 44.24% ($P < 0.05$; Fig. 4). The effect of microbe-derived POC on SOC sequestration still existed when C input increased. Along the C input gradient, the SOC difference between the two models was enlarged (Fig. S4). When DOC input increased by 20%, the SOC increases (normalized to their respective steady state) were 0.23 mg g^{-1} – 3.68 mg g^{-1} soil in Model I and 0.32 mg g^{-1} – 5.13 mg g^{-1} soil and Model II ($P < 0.05$, Fig. S5). Similarly, when both DOC and POC input increased by 20%, Model II produced a significantly greater SOC content than Model I (0.96 mg g^{-1} – 11.33 mg g^{-1} soil by Model II vs. 0.84 mg g^{-1} – 9.18 mg g^{-1} soil by Model I; $P < 0.05$, Fig. S5).

https://doi.org/10.5194/egusphere-2023-1483
Preprint. Discussion started: 25 July 2023

4 Discussion

4.1 Microbe-mediated formation of POC from dissolved C inputs

This study showed that most of labile C preferentially entered the MAOC pool, but still up to 12.29% of the glucose-C has become part of POC after the 102-day incubation. The results indicate that dissolved labile plant compounds (glucose in our case), in addition to structural litter, could be a significant contributor to POC. The result is supported by Sokol et al. (2019b), which finds that living root inputs are efficiency in forming both MAOC and POC. In addition, the POC formation positively correlated with the glucose-derived MBC (Fig. 3a), suggesting that the transformation of glucose to POC could be dependent on the microbe-mediated biochemical pathway. Meanwhile, the formation of POC is positively dependent on the fraction of clay and silt as well (R^2 = 0.92, Fig. 3b), further indicating POC formation is an interaction of physical and biochemical processes. These results are consistent with previous studies which showed the formation of heavy-POC (or coarse-MAOC) from microbial by-products binding with the silt- and clay-sized soil minerals (Samson et al., 2020). From a microscopic perspective, our result is supported by previous studies with images from scanning electron microscopy (SEM) and nano-scale secondary ion mass spectrometry (NanoSIMS), which show that microorganisms could absorb to the surface of particulate organic matter (POM) and bind it with mineral (Kopittke et al., 2020; Witzgall et al., 2021). The result that labile C can enter the POC pool are inconsistent with the two-pathway framework, which proposes that low-molecular-weight, water-soluble inputs contribute primarily to MAOC formation via the microbe-mediated biochemical pathway, whereas POC is formed primarily from the polymeric structural inputs via the physical transfer pathway (Cotrufo et al., 2015). Our results, combined with previous studies, demonstrate that the biochemical and physical pathways in SOC formation may not be independent with each other. Rather, the formations of POC and MAOC are continuous through close interactions of physical and microbial processes, during which POC formation from dissolved substrates is a critical component in SOC dynamics.

4.2 Effect of microbe-mediated POC formation on SOC sequestration

As POM surfaces are considered the hotspots of microbial activity and cores of aggregate formation (Tisdall and Oades, 1982; Witzgall et al., 2021), our modeling analyses indicated that dissolved substrates-originated POC formation can significantly influence long-term SOC sequestration. Although both Model I and Model II fitted the C flux data well, Model I, which does not include the C flow from MBC to POC, was not able to reproduce the observed POC changes (Fig. S3). The results emphasize the necessity of including the microbe-mediated POC formation in SOC dynamic models.

During the model calibration, including or not the C flow from MBC to POC significantly affected the estimations of turnover and transfer parameters. Specifically, the turnover rates of C pools were underestimated and transfer coefficients were overestimated by Model I compared with Model II (Table S3). This is because the absence of C flow from MBC to POC in Model I would allow more C to be allocated to respiration. To alleviate this phenomenon, the algorithm tended to mistakenly decrease their turnover and increase C allocation to other C pools to fit respiration flux data. As a result, the absence of mechanism of microbe-mediated POC formation can have a significant impact on the long-term prediction of SOC, leading to

https://doi.org/10.5194/egusphere-2023-1483
Preprint. Discussion started: 25 July 2023

an underestimation of SOC sequestration in Model I (Fig. 4). In addition, the underestimation of SOC sequestration would be exacerbated as the magnitude of C input increases (Fig. S4). These results indicate that the microbe-mediated POC formation is critical for long-term SOC sequestration and should be considered in soil C dynamic models.

5 Conclusions

This study provides direct evidence that dissolved labile C can not only contribute to MAOC formation, but also to POC formation, through the microbe-mediated biochemical pathway. As a result, dissolved plant compounds, in addition to structural litter, are vital contributors to POC. The microbe-mediated POC formation is a critical component in SOC dynamics. From the modeling perspective, ignoring the mechanism of microbe-mediated POC formation would cause a significant underestimation of long-term SOC sequestration.

Author contributions

Junyi Liang and Qintana Si designed the study. Yaowen Zhang, Xun Sun conducted the soil sampling. Qintana Si, Kangli Chen, and Bin Wei conducted the incubation experiment. Junyi Liang and Qintana Si developed the modeling framework. Junyi Liang and Qintana Si performed the analyses. All the authors contributed to writing the manuscript.

Acknowledgements

This study was financially supported by the National Natural Science Foundation of China (42203077, 32192462), the Chinese Universities Scientific Fund (2020RC009) and the 2115 Talent Development Program of China Agricultural University (1201-336 00109017).

Competing interests

The authors declare that they have no conflict of interest.

Data availability statement

All data will be freely available upon acceptance.

https://doi.org/10.5194/egusphere-2023-1483
Preprint. Discussion started: 25 July 2023

References

Bai, Y. F. and Cotrufo, M. F.: Grassland soil carbon sequestration: Current understanding, challenges, and solutions, Science, 377, 603-608, https://doi.org/10.1126/science.abo2380, 2022.

Baldock, J. A. and Skjemstad, J. O.: Role of the soil matrix and minerals in protecting natural organic materials against biological attack, Organic Geochemistry, 31, 697-710, https://doi.org/10.1016/s0146-6380(00)00049-8, 2000.

Basile-Doelsch, I., Balesdent, J., and Pellerin, S.: Reviews and syntheses: The mechanisms underlying carbon storage in soil, Biogeosciences, 17, 5223-5242, https://doi.org/10.5194/bg-17-5223-2020, 2020.

Benbi, D. K., Boparai, A. K., and Brar, K.: Decomposition of particulate organic matter is more sensitive to temperature than the mineral associated organic matter, Soil Biology and Biochemistry, 70, 183-192, https://doi.org/10.1016/j.soilbio.2013.12.032, 2014.

Chapin, F. S., III, Matson, P. A., Vitousek, P. M., and SpringerLink: Principles of terrestrial ecosystem ecology, Springer New York, New York, NY2011.

Cotrufo, M. F. and Lavallee, J. M.: Soil organic matter formation, persistence, and functioning: A synthesis of current understanding to inform its conservation and regeneration, Adv Agron, 172, 1-66, https://doi.org/10.1016/bs.agron.2021.11.002, 2022.

Cotrufo, M. F., Ranalli, M. G., Haddix, M. L., Six, J., and Lugato, E.: Soil carbon storage informed by particulate and mineral-associated organic matter, Nature Geoscience, 12, 989-+, https://doi.org/10.1038/s41561-019-0484-6, 2019.

Cotrufo, M. F., Wallenstein, M. D., Boot, C. M., Denef, K., and Paul, E.: The Microbial Efficiency-Matrix Stabilization (MEMS) framework integrates plant litter decomposition with soil organic matter stabilization: do labile plant inputs form stable soil organic matter?, Glob. Change Biol., 19, 988-995, https://doi.org/10.1111/gcb.12113, 2013.

Cotrufo, M. F., Soong, J. L., Horton, A. J., Campbell, E. E., Haddix, Michelle L., Wall, D. H., and Parton, W. J.: Formation of soil organic matter via biochemical and physical pathways of litter mass loss, Nature Geoscience, 8, 776-779, https://doi.org/10.1038/ngeo2520, 2015.

Haario, H., Saksman, E., and Tamminen, J.: An adaptive Metropolis algorithm, Bernoulli, 7, 223-242, https://doi.org/10.2307/3318737, 2001.

Hararuk, O., Xia, J. Y., and Luo, Y. Q.: Evaluation and improvement of a global land model against soil carbon data using a Bayesian Markov chain Monte Carlo method, Journal of Geophysical Research-Biogeosciences, 119, 403-417, https://doi.org/10.1002/2013jg002535, 2014.

Kleber, M., Eusterhues, K., Keiluweit, M., Mikutta, C., and Nico, P. S.: Mineral–Organic Associations: Formation, Properties, and Relevance in Soil Environments, Advances in Agronomy, 130, 1-140, 2015.

Kopittke, P. M., Dalal, R. C., Hoeschen, C., Li, C., Menzies, N. W., and Mueller, C. W.: Soil organic matter is stabilized by organo-mineral associations through two key processes: The role of the carbon to nitrogen ratio, Geoderma, 357, https://doi.org/10.1016/j.geoderma.2019.113974, 2020.

https://doi.org/10.5194/egusphere-2023-1483
Preprint. Discussion started: 25 July 2023

Lavallee, J. M., Soong, J. L., and Cotrufo, M. F.: Conceptualizing soil organic matter into particulate and mineral-associated forms to address global change in the 21st century, Glob. Change Biol., 26, 261-273, https://doi.org/10.1111/gcb.14859, 2020.

Lehmann, J., Hansel, C. M., Kaiser, C., Kleber, M., Maher, K., Manzoni, S., Nunan, N., Reichstein, M., Schimel, J. P., Torn, M. S., Wieder, W. R., and Kogel-Knabner, I.: Persistence of soil organic carbon caused by functional complexity, Nature Geoscience, 13, 529-534, https://doi.org/10.1038/s41561-020-0612-3, 2020.

Li, J., Wang, G., Allison, S. D., Mayes, M. A., and Luo, Y.: Soil carbon sensitivity to temperature and carbon use efficiency compared across microbial-ecosystem models of varying complexity, Biogeochemistry, 119, 67-84, https://doi.org/10.1007/s10533-013-9948-8, 2014.

Liang, C., Schimel, J. P., and Jastrow, J. D.: The importance of anabolism in microbial control over soil carbon storage, Nature Microbiology, 2, 17105, https://doi.org/10.1038/nmicrobiol.2017.105, 2017.

Liang, J. Y., Li, D. J., Shi, Z., Tiedje, J. M., Zhou, J. Z., Schuur, E. A. G., Konstantinidis, K. T., and Luo, Y. Q.: Methods for estimating temperature sensitivity of soil organic matter based on incubation data: A comparative evaluation, Soil Biology and Biochemistry, 80, 127-135, https://doi.org/10.1016/j.soilbio.2014.10.005, 2015.

Lugato, E., Lavallee, J. M., Haddix, M. L., Panagos, P., and Cotrufo, M. F.: Different climate sensitivity of particulate and mineral-associated soil organic matter, Nature Geoscience, 14, 295-300, https://doi.org/10.1038/s41561-021-00744-x, 2021.

Mikutta, R., Turner, S., Schippers, A., Gentsch, N., Meyer-Stuve, S., Condron, L. M., Peltzer, D. A., Richardson, S. J., Eger, A., Hempel, G., Kaiser, K., Klotzbucher, T., and Guggenberger, G.: Microbial and abiotic controls on mineral-associated organic matter in soil profiles along an ecosystem gradient, Scientific Reports, 9, https://doi.org/10.1038/s41598-019-46501-4, 2019.

Prater, I., Zubrzycki, S., Buegger, F., Zoor-Fullgraff, L. C., Angst, G., Dannenmann, M., and Mueller, C. W.: From fibrous plant residues to mineral-associated organic carbon - the fate of organic matter in Arctic permafrost soils, Biogeosciences, 17, 3367-3383, https://doi.org/10.5194/bg-17-3367-2020, 2020.

Robertson, A. D., Paustian, K., Ogle, S., Wallenstein, M. D., Lugato, E., and Cotrufo, M. F.: Unifying soil organic matter formation and persistence frameworks: the MEMS model, Biogeosciences, 16, 1225-1248, https://doi.org/10.5194/bg-16-1225-2019, 2019.

Samson, M.-É., Chantigny, M. H., Vanasse, A., Menasseri-Aubry, S., and Angers, D. A.: Coarse mineral-associated organic matter is a pivotal fraction for SOM formation and is sensitive to the quality of organic inputs, Soil Biology and Biochemistry, 149, https://doi.org/10.1016/j.soilbio.2020.107935, 2020.

Sokol, N. W., Sanderman, J., and Bradford, M. A.: Pathways of mineral-associated soil organic matter formation: Integrating the role of plant carbon source, chemistry, and point of entry, Glob. Change Biol., 25, 12-24, https://doi.org/10.1111/gcb.14482, 2019a.

Sokol, N. W., Kuebbing, S. E., Karlsen-Ayala, E., and Bradford, M. A.: Evidence for the primacy of living root inputs, not root or shoot litter, in forming soil organic carbon, New Phytologist, 221, 233-246, https://doi.org/10.1111/nph.15361, 2019b.

https://doi.org/10.5194/egusphere-2023-1483
Preprint. Discussion started: 25 July 2023

Tisdall, J. M. and Oades, J. M.: Organic-Matter and Water-Stable Aggregates in Soils, J Soil Sci, 33, 141-163, https://doi.org/10.1111/j.1365-2389.1982.tb01755.x, 1982.

Vance, E. D., Brookes, P. C., and Jenkinson, D. S.: An Extraction Method for Measuring Soil Microbial Biomass-C, Soil Biology and Biochemistry, 19, 703-707, https://doi.org/10.1016/0038-0717(87)90052-6, 1987.

White, R. P., Murray, S., Rohweder, M., Prince, S. D., and World Resources, I.: Pilot analysis of global ecosystems: grassland ecosystems, World Resources Institute, Washington, DC2000.

Wiesmeier, M., Urbanski, L., Hobley, E., Lang, B., von Lutzow, M., Marin-Spiotta, E., van Wesemael, B., Rabot, E., Liess, M., Garcia-Franco, N., Wollschlager, U., Vogel, H. J., and Kogel-Knabner, I.: Soil organic carbon storage as a key function of soils - A review of drivers and indicators at various scales, Geoderma, 333, 149-162, https://doi.org/10.1016/j.geoderma.2018.07.026, 2019.

Witzgall, K., Vidal, A., Schubert, D. I., Hoschen, C., Schweizer, S. A., Buegger, F., Pouteau, V., Chenu, C., and Mueller, C. W.: Particulate organic matter as a functional soil component for persistent soil organic carbon, Nature Communications, 12, https://doi.org/10.1038/s41467-021-24192-8, 2021.

Table 1: Information of the sampling sites and soil physical and chemical properties (mean±standard error).

Site	Fencing treatment	Abbrev-iation	Longitude (°E)	Latitude (°N)	Altitude (m)	Mean annual precipit-ation (mm)	Mean annual temper-ature (°C)	Clay (%)	Silt (%)	Sand (%)	pH	SOC (g kg^{-1})	MBC (mg kg^{-1})	DOC (mg kg^{-1})
DL	fencing	DL_{in}	116.27	42.06	1306.22	378.00	3.30	9.4	17.7	71.3	7.52±0.07	57.08±3.53	454.36±25.91	94.45±3.03
DL	grazing	DL_{out}						10.3	18.3	67.2	7.27±0.20	59.70±1.62	487.63±32.24	85.74±8.34
GY	fencing	GY_{in}	115.59	41.78	1391.95	398.40	-1.40	9.2	20.1	70.6	8.02±0.21	40.13±2.67	567.96±8.90	137.92±1.22
GY	grazing	GY_{out}						10.0	14.9	74.1	7.57±0.16	31.88±0.76	432.34±28.38	101.79±3.90
HL	fencing	HL_{in}	120.16	49.44	673.95	352.00	-0.10	5.5	40.3	53.0	6.29±0.12	37.01±1.95	606.85±104.34	61.89±35.81
HL	grazing	HL_{out}						14.2	24.6	59.2	6.43±0.08	29.04±1.81	182.33±24.70	189.27±10.82
XL	fencing	XL_{in}	116.74	43.60	1198.22	263.50	3.50	5.9	8.7	83.4	6.65±0.16	12.27±1.03	253.70±5.21	43.34±1.40
XL	grazing	XL_{out}						8.6	5.0	84.5	6.60±0.19	9.00±0.60	183.22±7.43	21.97±3.09
XH	fencing	XH_{in}	114.09	42.37	1224.96	270.60	4.20	4.1	5.8	75.9	7.40±0.15	7.84±0.65	127.43±0.50	48.00±1.35
XH	grazing	XH_{out}						4.8	10.9	75.0	7.65±0.13	7.02±0.80	209.73±6.83	54.31±3.45

https://doi.org/10.5194/egusphere-2023-1483
Preprint. Discussion started: 25 July 2023

https://doi.org/10.5194/egusphere-2023-1483
Preprint. Discussion started: 25 July 2023

303 **Table 2: Description of the soil carbon (C) model parameters.**

304

Parameter	Description	Unit
f_P	Initial fraction of the POC pool	-
k_D	Turnover rate of the DOC pool	mg C g^{-1} soil h^{-1}
k_B	Turnover rate of the MBC pool	mg C g^{-1} soil h^{-1}
k_P	Turnover rate of the POC pool	mg C g^{-1} soil h^{-1}
k_M	Turnover rate of the MAOC pool	mg C g^{-1} soil h^{-1}
f_{MB}	MBC to MAOC transfer coefficient	-
f_{MP}	POC to MAOC transfer coefficient	-
f_{PB}	MBC to POC transfer coefficient (only exist in model II)	-
f_{DP}	POC to DOC transfer coefficient	-
f_{DM}	MAOC to DOC transfer coefficient	-
f_{BD}	DOC to MBC transfer coefficient	-

https://doi.org/10.5194/egusphere-2023-1483
Preprint. Discussion started: 25 July 2023

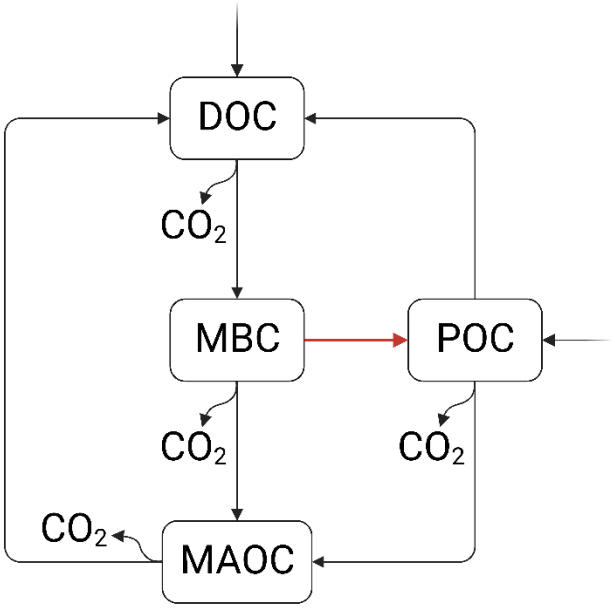

305

306 **Figure 1: The model scheme of soil carbon (C) dynamics.** Model I and Model II share similar structure except that Model II includes a C
307 flow from MBC to POC (red arrow) but Model I does not.

308

https://doi.org/10.5194/egusphere-2023-1483
Preprint. Discussion started: 25 July 2023

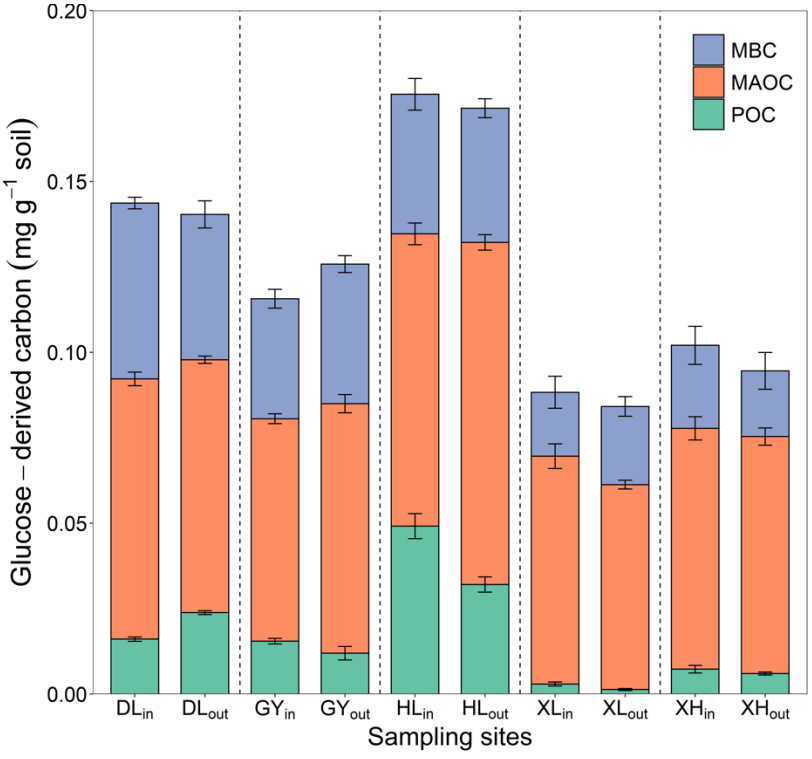

Figure 2: Distributions of glucose-derived C in soil C pools. The error bars represent the standard errors of four replicates. microbial biomass C: MBC, mineral-associated organic C: MAOC, particulate organic C: POC.

https://doi.org/10.5194/egusphere-2023-1483
Preprint. Discussion started: 25 July 2023

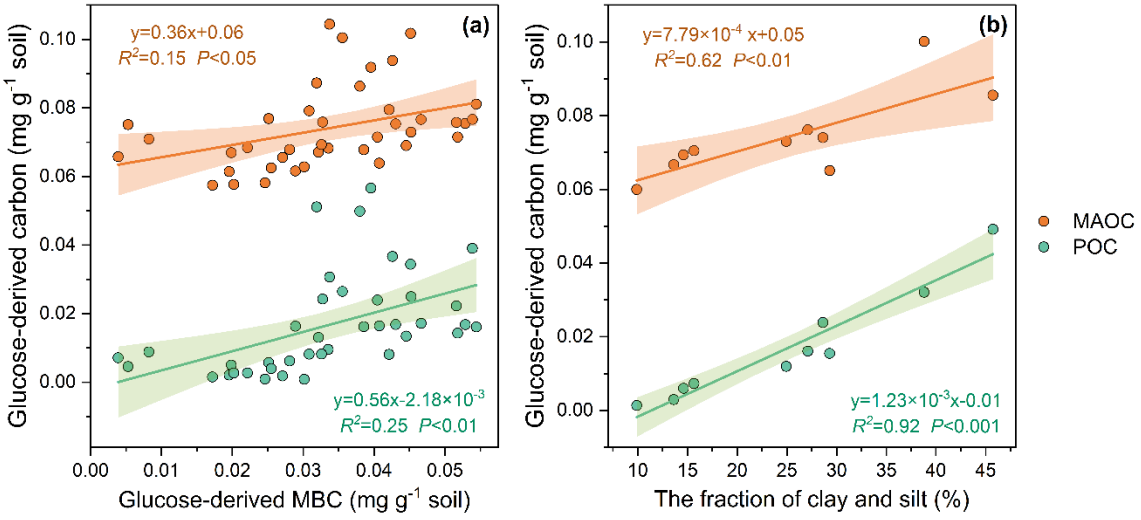

Figure 3: Dependence of glucose-derived POC and MAOC on MBC (a) and soil texture (b). Shaded areas represent the 95% confidence intervals for the regression lines.

https://doi.org/10.5194/egusphere-2023-1483
Preprint. Discussion started: 25 July 2023

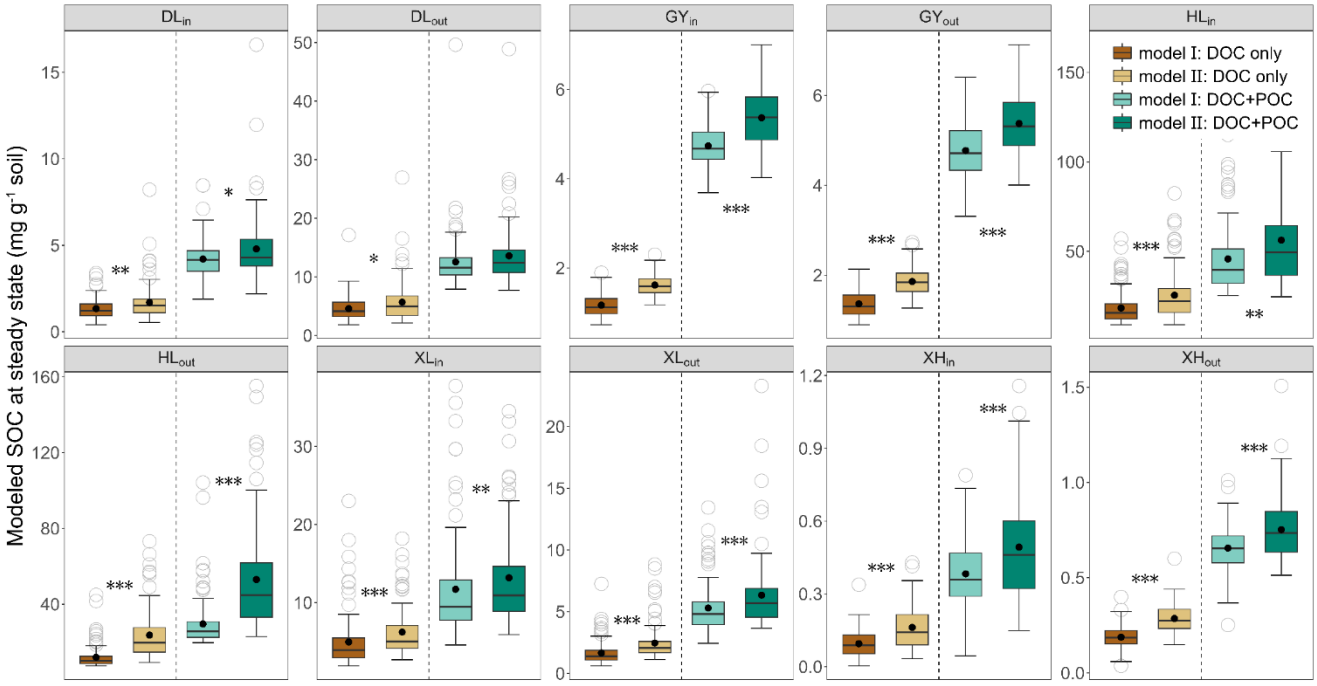

Figure 4: Modeled SOC content at steady state under two types of C input conditions. The upper and lower ends of boxes denote the 0.25 and 0.75 percentiles, respectively. The solid line and solid dots in the box mark the median and mean of each dataset. Hollow dot denotes outliers. Asterisks represent significant differences between Model I and Model II (*P < 0.05, **P < 0.01, ***P < 0.001).